Exp. Eye Res. (2002) **74**, 677–687
doi:10.1006/exer.2001.1164, available online at http://www.idealibrary.com on IDEAL®

Anisotropic Water Transport in the Human Eye Lens Studied by Diffusion Tensor NMR Micro-imaging

B. A. MOFFAT AND J. M. POPE*

Centre for Medical, Health and Environmental Physics, Queensland University of Technology, GPO Box 2434, Brisbane, Queensland 4001, Australia

(*Received Norwich 30 July 2001 and accepted in revised form 14 November 2001*)

We report in vitro measurements of effective diffusion tensors characterising the anisotropic transport of water in human eye lenses ranging in age from 13 to 86 years. The measurements were obtained by means of a pulsed field gradient spin echo (PFGSE) magnetic resonance imaging (MRI) technique at a spatial resolution of $218 \times 218 \times 1000\ \mu m^3$. The results show that water diffusion is both spatially inhomogeneous and highly anisotropic on the timescale of the measurements (approximately 15 msec). Diffusion parallel to the long axes of the lens fibre cells is relatively unrestricted, whereas that between cells is substantially inhibited by the cell membranes, particularly in the inner cortex region of the lens. The data confirm the presence of a diffusion barrier surrounding the lens nucleus, which inhibits transport of water and other small molecules into and out of the nucleus. The results shed light on factors that may influence the onset of presbyopia and senile cataract. They also have implications for delivery of drugs to the lens nucleus.

Key words: eye lens; diffusion tensor; water transport; magnetic resonance, imaging; senile cataract.

1. Introduction

In order to perform its functions, the human eye lens must combine transparency and a high refractive index with flexibility to facilitate accommodation. The lens is a syncytium of fibre cells that are connected by gap junctions, ion channels and water channels. The lens fibre cells have a high protein (crystallin) content (> 30 %) and there is very little extra-cellular water (Paterson, 1970) resulting in a refractive index that is typically in the range between approximately 1·36 and 1·42. Most of the cells also contain no organelles, which minimize light scattering. However, the lack of organelles makes mature lens fibre cells vulnerable to insult because there are limited, if any, mechanisms for repairing or replacing damaged proteins or membranes.

The inner lens fibre cells rely on the transport of water-soluble nutrients (Mathias et al., 1997) and anti-oxidants such as glutathione (Sweeney and Truscott, 1998) from the metabolically active outer cortex and epithelial cells into the lens nucleus. The maintenance of lens homeostasis is, therefore, a fine balance between oxidative (Truscott and Augusteyn, 1977; Bron et al., 2000) and glycolitic (Cheng et al., 1985; Gonzalez et al., 1986; Hightower and Harrison, 1987; Tsubota et al., 1989; Tsubota and Laing, 1992; Obrosova et al., 1997) stress prevention and repair mechanisms. With no vascular system and little extra-cellular water, transport of water and water-soluble metabolites through water channels such as aquaporins and gap junctions (Goodenough, 1992; Mathias et al., 1997) is vital for maintaining the condition of the lens.

Transport rate data are not only important for understanding the transport mechanisms, but also necessary for developing pharmacological solutions to cataract. It is known that the lens readily takes up pharmaceuticals such as aldose reductase inhibitors (Ohtori et al., 1991); however, their rate of transport into the lens nucleus is unknown. The detailed nature of the transport mechanism itself is also unknown, although it is likely to be via passive diffusion or convective flow caused by ion currents through the lens's network of gap junctions and aquaporins (Mathias et al., 1997).

Sweeney and Truscott 1998) used a radioactive-labelling technique to study the transport of glutathione (GSH) into the lens nucleus. The concentration of radio-labelled GSH in the lens nucleus was found to be significantly lower in older lenses despite adequate uptake by the lens cortex. The authors proposed that a barrier to the transport of GSH into the lens nucleus developed during the ageing of the lens. It was reported that the size of the barrier region correlated closely with the dimensions of nuclear cataracts found in the population.

Although water itself does not contain any anti-oxidant or nutrient properties for the lens cells, it is fundamental to the health of the lens. It is the solvent for all the metabolites and crystallins within the lens cells. Therefore, it provides the medium for vital chemical reactions, as well as transport of metabolites and waste products. The substantial number of gap junctions and aquaporins (Goodenough, 1992) in the

* Author for correspondence. E-mail: j.pope@qut.edu.au

0014-4835/02/$35.00/0

lens together with evidence from ion transport studies (Mathias et al., 1997) indicates that the transport of water is vitally important to the homeostasis of the lens.

In a previous in vitro study (Moffat et al., 1999) of human eye lenses, we used a D_2O substitution technique to study the exchange of water into and out of the lens nucleus as a function of lens age. The results were consistent with a threefold reduction of the effective self-diffusion coefficient for water in the lens from approximately $2{\cdot}2 \times 10^{-10}$ m^2 s^{-1} in young lenses to approximately $0{\cdot}7 \times 10^{-10}$ m^2 s^{-1} in the oldest lenses studied. However, while the data showed no evidence for convective flows as suggested by Mathias et al. (1997), the results were unable to distinguish the extent of any anisotropy in the water transport on the scale of the lens fibre cell dimensions.

In this paper, we report in vitro NMR micro-imaging measurements of diffusion tensors characterizing the anisotropic transport of water in human eye lenses ranging in age from 13 to 86 years. NMR measurements of self-diffusion are advantageous because they measure the diffusion process in the absence of a concentration gradient and without the need for solution of the diffusion equation for complex geometries. It should be emphasized, however, that the method measures effective diffusion coefficients which may include contributions from active transport or convective flows provided only that the flow is incoherent on the scale of the image voxel dimensions (intra-voxel incoherent motion). Lens water self-diffusion has been previously measured by non-imaging methods (Haner et al., 1989; Babizhaev et al., 1991). The results showed that there is significant restriction of water diffusion in the lens and suggested that there are multiple pools of water with different diffusion coefficients. However, the origin of the restriction and the multiple components was not determined in these studies.

2. Methods

Human lenses were acquired from both the Queensland and NSW Eye Banks, where they were removed from the eyes of donors and immediately transferred to artificial aqueous humour (AAH) containing nutrients and metabolites similar to those present in vivo. The AAH was made up from Auto-Pow minimum essential medium-Earls (MEME) salts, (ICN Biochemicals, Costa Mesa, CA), with the addition of HEPES (10 mM), glutamine (2 mM), penicillin (1000 μg l^{-1}), streptomycin (1 mg l^{-1}) amphotericin (10 mg l^{-1}) and adjusted to a pH of 7·4. Lenses were maintained at 34·5°C and transported to the laboratory within 48 hours after death of the donor. They were then transferred to an NMR tube containing AAH ready for imaging and maintained at 34·5°C throughout the ensuing measurements.

Diffusion Tensor Imaging

Diffusion of nuclear spins in the presence of an applied linear magnetic field gradient results in a phase dispersion and attenuation of the NMR signal, analogous to that resulting from transverse relaxation (T_2). Stejskal and Tanner (1965) showed that by modifying the standard spin echo sequence to incorporate a 'bipolar' gradient in the form of two consecutive gradient pulses of duration δ and separation Δ, the signal attenuation is given by

$$S = S_0\, e^{-T_E/T_2}\, e^{-\gamma^2 G^2 D \delta^2 (\Delta - \delta/3)} = S_0'\, e^{-bD},$$

where

$$S_0' = S_0\, e^{-T_E/T_2} \text{ and } b = \gamma^2 G^2 \delta^2 (\Delta - \delta/3).$$

By keeping the echo time T_E fixed and incrementing the amplitude of the magnetic field gradient pulses (G) in such a pulsed field gradient spin echo (PFGSE) experiment, the self-diffusion coefficient (D) of the water protons can be determined.

Diffusion tensor images of human lenses were acquired on our Bruker 4·7 T micro-imaging system using a pulse sequence (Fig. 1) that separates the diffusion weighting from the imaging segment. This has the advantage that 'cross coupling' between the imaging and diffusion gradients (which can be significant in NMR micro-imaging because of the need for relatively large imaging gradients) is avoided. Images were acquired with a slice thickness of 1 mm through the symmetry axis of the lens, using a field of view of 28 mm comprising 128×128 pixels. Four averages were acquired per phase-encoding step, with a recycle time $T_R = 2$ sec, giving a total imaging time of approximately 2 hr for the complete data set. Diffusion gradient pulses of maximum amplitude $G = 0{\cdot}588$ T m^{-1} duration $\delta = 2{\cdot}5$ msec and separation $\Delta = 14{\cdot}5$ msec were employed, yielding a b-value of $1{\cdot}857 \times 10^9$ sec^{-2} and an echo time $T_E \approx 27$ ms. Thus, we are measuring diffusion on a timescale Δ corresponding to diffusion lengths for water of order 10 μm which are comparable to the cell dimensions. As the cells are fibre-like in shape with diameter approximately 6–8 μm, extending from pole to pole in the cortex, we would expect to observe diffusion anisotropy on this timescale.

Computation and Display of Data

A significant problem in diffusion tensor imaging is how best to display the resulting images and relate the results to the sample morphology, because in general, each pixel in a diffusion tensor image is characterized by six parameters. However, provided that the image plane was chosen to coincide with the symmetry plane through the optical axis of the lens, so that the long axes of the lens fibre cells lay predominantly in

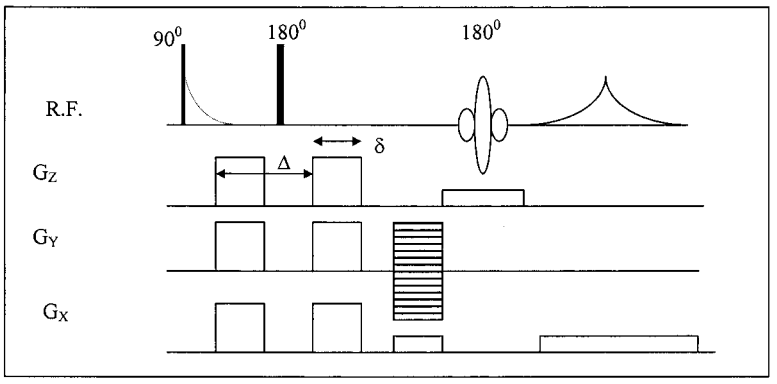

FIG. 1. Pulse field gradient spin echo imaging (PFGSEI) sequence. The magnetic field gradient pulses applied symmetrically with respect to the first (non-selective) 180° radiofrequency (RF) pulse are used to diffusion-weight the magnetization of the sample, prior to application of the imaging gradients. The effective diffusion time Δ was 14·5 msec.

the image plane, the off-diagonal elements D_{xz} and D_{yz} of the raw (un-diagonalized) diffusion tensor invariably contained little signal (see, for example, the top images of Fig. 2). This implies that the z direction (which was normal to the image plane) corresponded closely to one of the principal axes of the diffusion tensor and in this case diagonalization involves a simple rotation about z.

This 'a priori' knowledge means that, in the principal axes frame, we can describe the diffusion in terms of a 2×2 tensor whose diagonal elements designated as D_{para} and D_{perp}, corresponding to diffusion parallel and perpendicular to the direction of maximum diffusivity in the plane of the image slice, respectively. Further, only one angle θ is required to describe the orientation of the principal axis of the diffusion tensor with respect to the gradient axes. Consequently, we only require four images to calculate D_{para}, D_{perp} and θ, corresponding to gradients of 0, G_x, G_y and $(G_x + G_y)/\sqrt{2}$ (Coremans et al., 1994). This

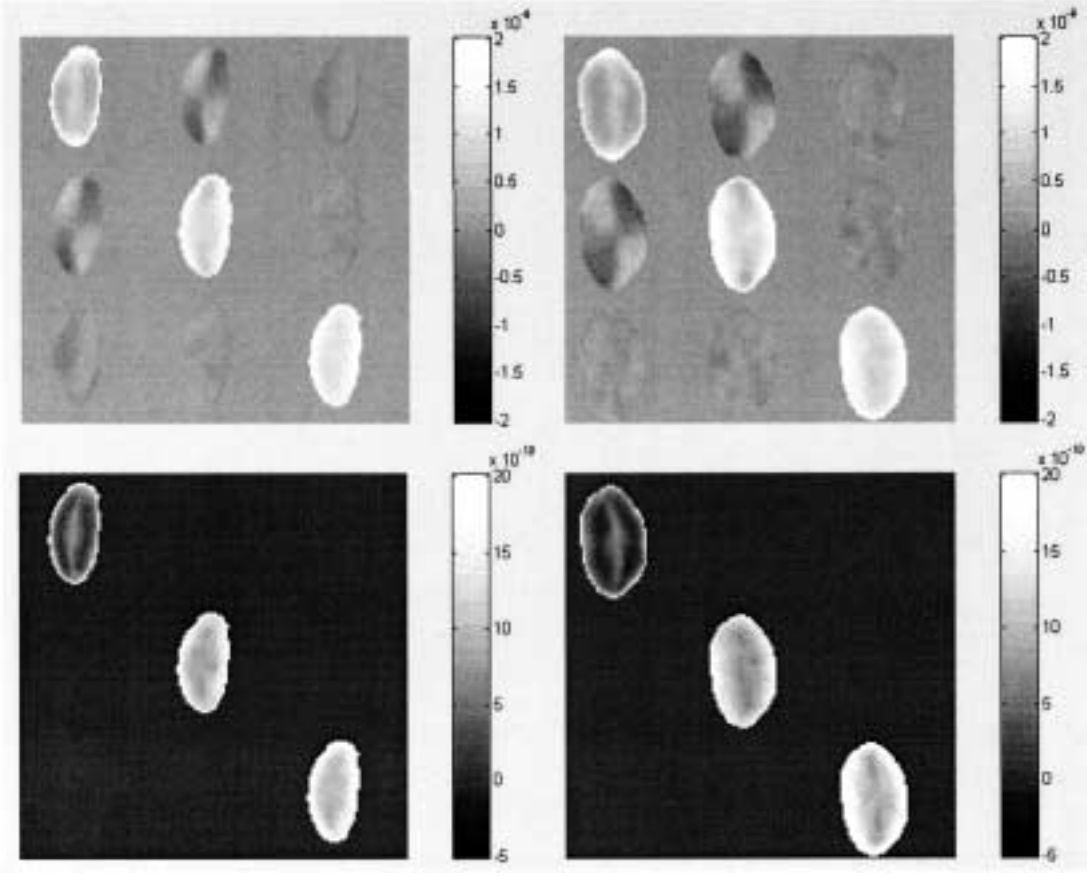

FIG. 2. Diffusion tensor maps of a 29 year old (left) and an 86 year old (right) human eye lens. The nine images in each diffusion tensor map correspond to the nine elements of the full 3×3 diffusion tensor. The top row represents the raw diffusion tensors (obtained directly from the ADC maps) and the bottom row the diagonalized (eigenvalue) maps. The scales are in units of m^2 sec^{-1}. In order to make the tensor maps clearer, the diffusion values of the water in the AAH have been set to 0.

provides a substantial reduction in overall imaging time and greatly simplifies the problem of how to display the resulting image data. The method we have developed for displaying the diffusion images makes use of the 'quiver plot' facility in Matlab® to generate, for each pixel, a pair of orthogonal lines whose lengths are proportional to D_{para} and D_{perp}, respectively, with the direction of the larger component defining the angle θ.

In general, the diffusion tensor and eigenvalues can be further simplified to a mean diffusivity. The mean diffusivity is rotationally invariant and is easily calculated from the trace of the diffusion tensor:

$$\overline{D} = \frac{1}{3}(D_{xx} + D_{yy} + D_{zz}).$$

However, it should be emphasized that the directional information characteristic of anisotropic diffusion is lost in calculating the mean diffusivity. As will be seen, this directional information is important in understanding the nature of water transport in the eye lens.

3. Results

Fig. 2 compares the diffusion tensor map for a lens from a 29 year old with that from an 86 year old donor. The top images are 3×3 diffusion tensor maps calculated directly from apparent diffusion coefficient (ADC) images using the procedure described, for example, by Coremans et al. (1994). In order to make the images clearer, the (isotropic) diffusion of water in the AAH surrounding the lenses has been artificially set to zero. The bottom images in Fig. 2 are the corresponding diagonalized (eigenvalue) maps, sorted such that $D_{33} > D_{22} > D_{11}$ where D_{11}, D_{22} and D_{33} are the principal components of the diagonalized diffusion tensor.

Diagonalized 2×2 diffusion tensor maps obtained from the same raw data are shown in Fig. 3. Here we have shown only the maps of the diagonal elements D_{perp} and D_{para}, together with profiles along the optical axis through the centre of the lens in each case. The images of Fig. 3 are virtually indistinguishable from the corresponding elements D_{11} and D_{33} respectively, shown in the lower images of Fig. 2. Fig. 4 shows a comparison of the mean diffusivity maps for the 29 year old and 86 year old lenses, together with corresponding profiles along the optical axis in each case.

Fig 5–7 are 'quiver plots' of the 2D diffusion tensors for the same two lenses. Fig. 5 shows both principal components D_{para} and D_{perp}, for comparison of their relative magnitudes, while Fig. 6 and 7 are plots of the maximum diffusivity D_{para} and minimum diffusivity D_{perp}, respectively. In the case of the full quiver plots of Fig. 5, the problem of sorting bias (Martin et al., 1999; Skare et al., 2000) is removed because both principal eigenvalues are displayed simultaneously. However, the plots of Fig. 6 and 7 are useful because they emphasize the spatial variations in direction and

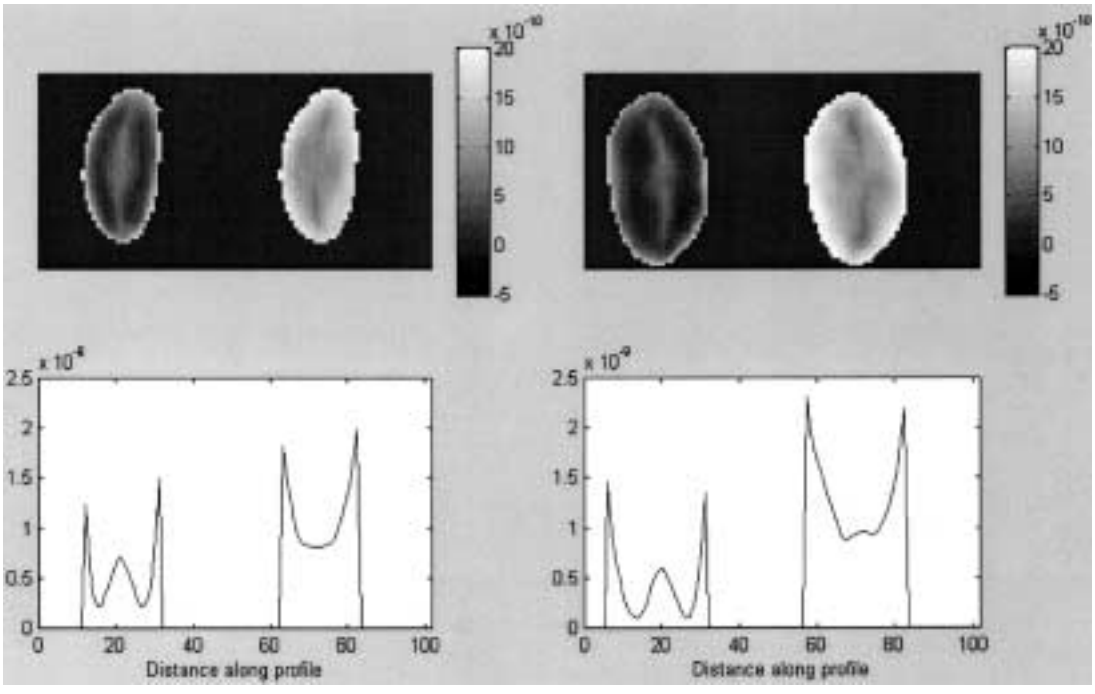

FIG. 3. Maps of the principal components D_{perp} (left) and D_{para} (right) of the diagonalised diffusion tensor obtained by treating the tensor as a 2×2 matrix. The images are derived from the same data as Fig. 2. Results on the left are from the 29 year old lens, and on the right from the 86 year old lens. These images are almost indistinguishable from those corresponding to the principal components D_{11} and D_{33} respectively, of Fig. 2. Profiles taken along the optical (symmetry) axis of the lens are shown below each image (with horizontal scales in pixels).

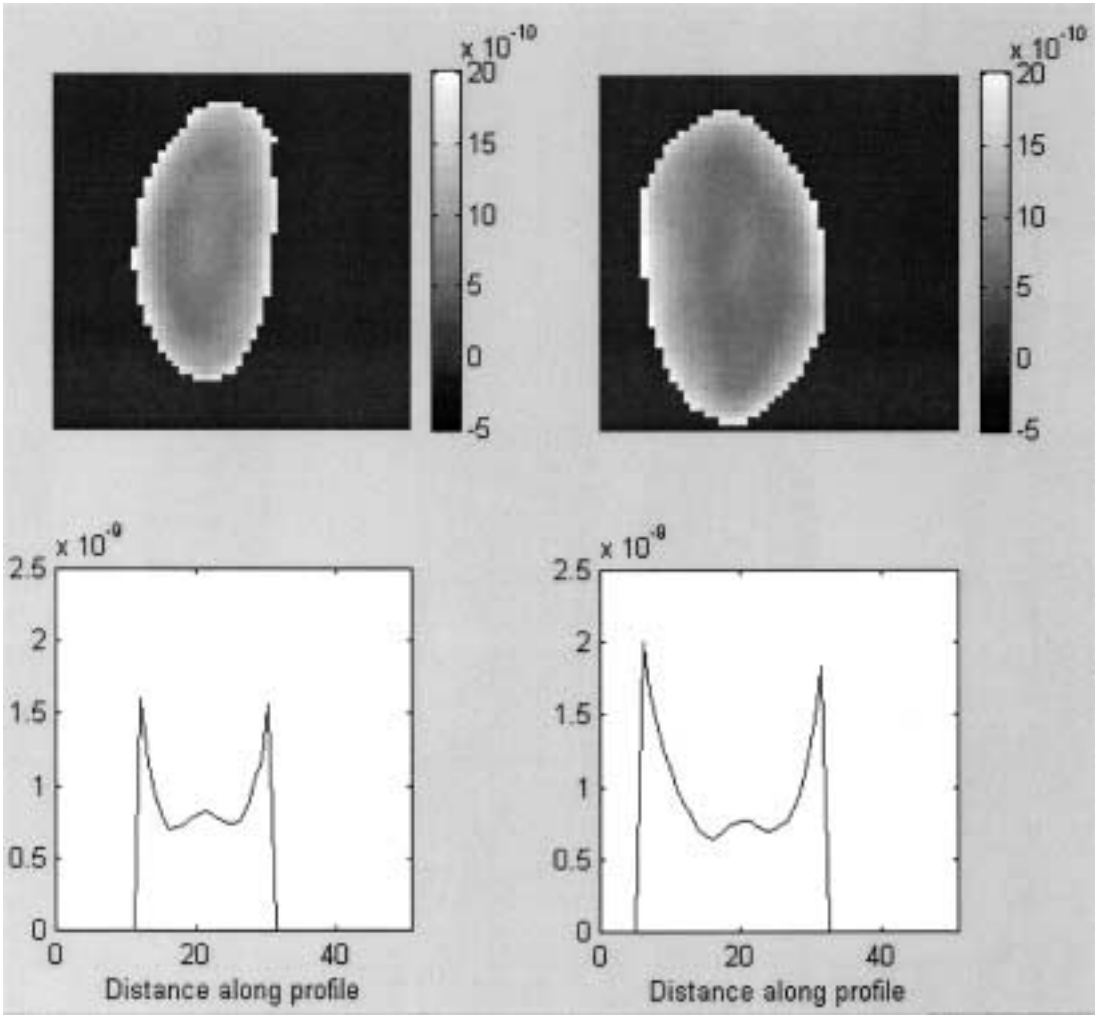

FIG. 4. Mean diffusivity maps (m^2 sec^{-1}) of the 29 year old lens (left) and the 86 year old lens (right) together with profiles taken along the optical axis in each case (with horizontal scale in pixels).

magnitude of the maximum and minimum eigenvalues, respectively.

4. Discussion

The images of Fig. 2 confirm that the diffusion of water in human eye lenses is highly anisotropic and inhomogeneous on the timescale of our measurements ($\Delta = 14{\cdot}5$ msec), as evidenced by the significant differences between the principal components D_{11}, D_{22} and D_{33} of the diagonalized diffusion tensors. This is further emphasized by the profiles across the maps of D_{para} and D_{perp} in Fig. 3. Both the maximum and minimum diffusivities show a substantial decrease between the lens surface and the nucleus, with the perpendicular diffusivity D_{perp} exhibiting a marked minimum in the inner cortex region. The mean diffusivity (Fig. 4) also exhibits a local minimum in a region surrounding the nucleus, although less marked than that of D_{perp}. The results are also indicative of the changes in size and shape that we typically observed between young and old lenses.

Inspection of the quiver maps of Fig. 5 shows that, in almost all pixels, the eigenvectors corresponding to the maximum or 'parallel diffusion' eigenvalues (D_{para}) are approximately parallel to the known direction of the long axes of the lens fibre cells, which tend to follow the contours of the lens surface. Conversely, the eigenvectors corresponding to the minimum or 'perpendicular diffusion' eigenvalues (D_{perp}) tend to be perpendicular to the lens fibre cell axes. As there is little extra-cellular water in the lens, these results indicate that diffusion of water is substantially constrained by the outer membranes of the lens fibre cells, but is relatively free within the cells themselves. The difference between D_{perp} and D_{para} is greatest in the middle cortical regions of the lens, indicating highest diffusion anisotropy occurs in this region. In the nucleus, the difference is reduced, but the anisotropy is still significant. In the pixels corresponding to the surface of the lens, diffusion appears isotropic and significantly higher than that in the lens cortex.

The separate quiver maps of D_{para} and D_{perp} shown in Fig. 6 and 7, respectively, allow comparison of the principal components of the diffusion tensor corresponding to the directions of most restricted and least restricted diffusion within the plane of the image slice.

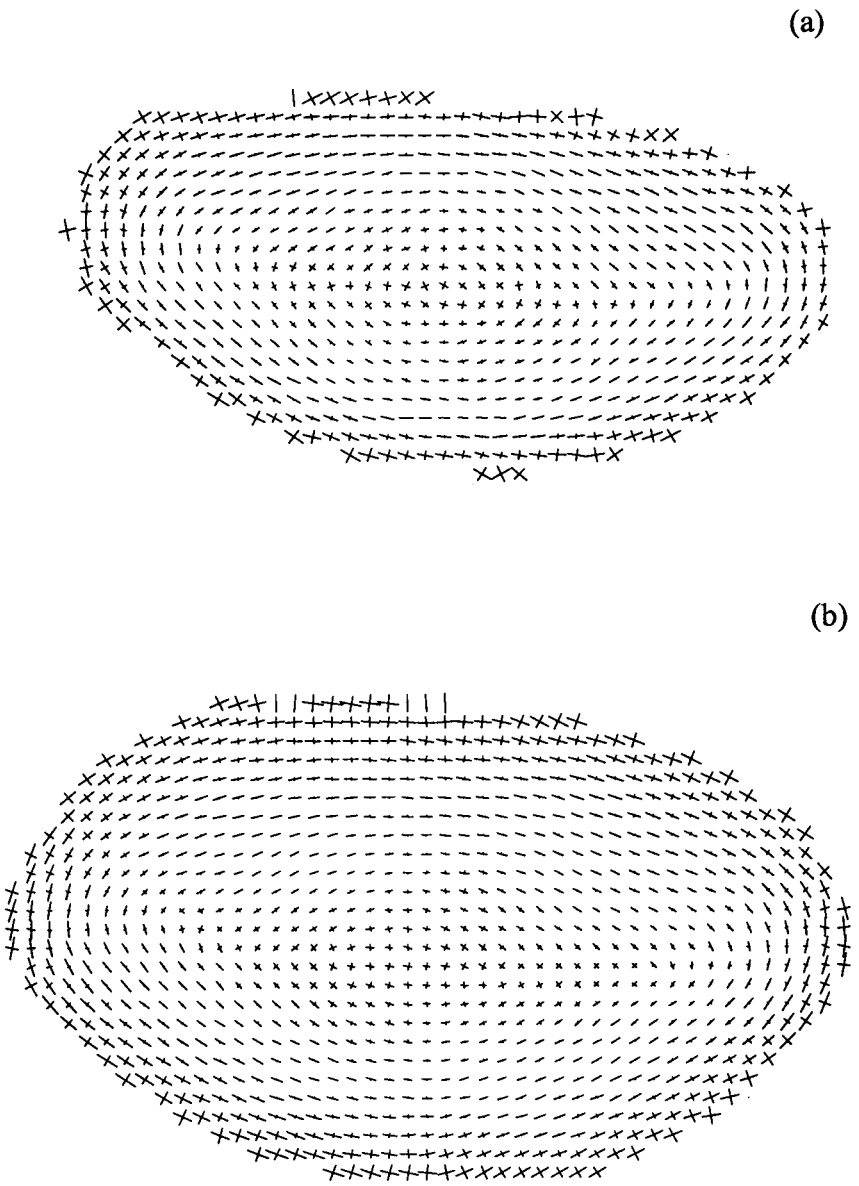

FIG. 5. Quiver plots of 2D diffusion tensors for a 29 year old lens (a) and an 86 year old lens (b). The vectors represent the direction and magnitude of the minimum and maximum diffusion ellipsoid principal axes in each pixel.

Inspection of these plots shows that both D_{para} and D_{perp} are strongly dependent on the radial distance from the lens centre. The magnitude of D_{para} is highest at the lens surface and smallest in the lens nucleus. This reflects the known difference in cytoplasm viscosity between nuclear and cortical fibre cells (Morgan et al., 1989). In nearly all lens fibre cells, the distance between cell membranes in the direction of D_{para} (cell lengths, approximately1–10 mm) is at least an order of magnitude greater than the mean squared displacement of the water molecules during the diffusion time Δ. Therefore D_{para} is a measure of the diffusion coefficient of water within the fibre cell cytoplasm.

The maps of D_{perp} (Fig. 7) exhibit a similar pattern to the maps of mean diffusivity (Fig. 4). However, the D_{perp} maps have a much steeper negative gradient than D_{para} within the lens cortex. As indicated previously, a distinct minimum in D_{perp} exists in a region surrounding the lens nucleus. D_{perp} then increases toward the centre of the lens nucleus. The region of most restricted diffusion is present in both young and old human lenses. The distances between cell membranes in the (radial) direction of D_{perp}, corresponding to the fibre cell thickness (approximately 6–8 μm), are of the same order as the root mean squared displacement of water molecules during the diffusion time Δ, indicating that this

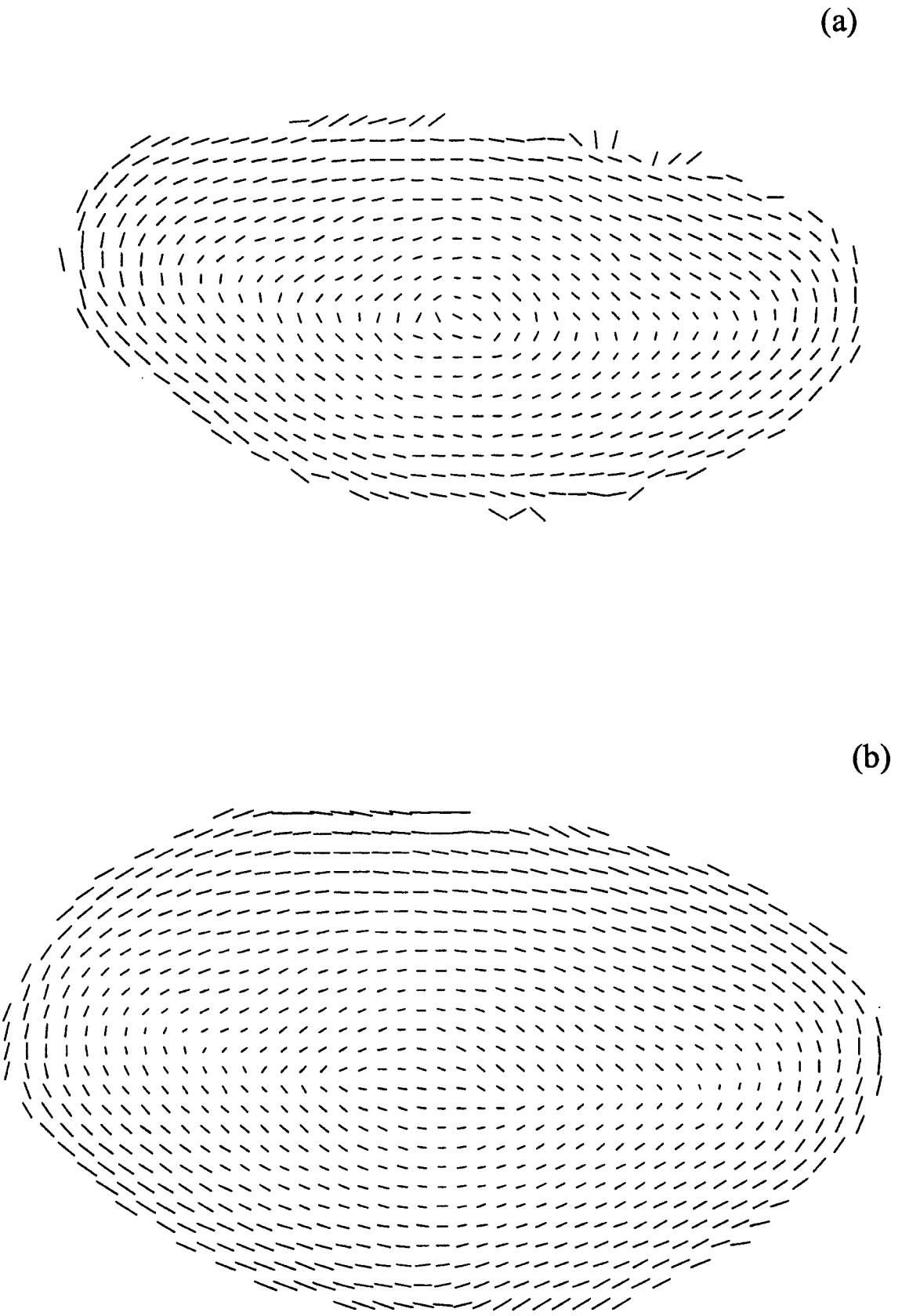

FIG. 6. Quiver plots of the largest component of the diagonalised diffusion tensor D_{para} for a 29 year old lens (a) and an 86 year old lens (b).

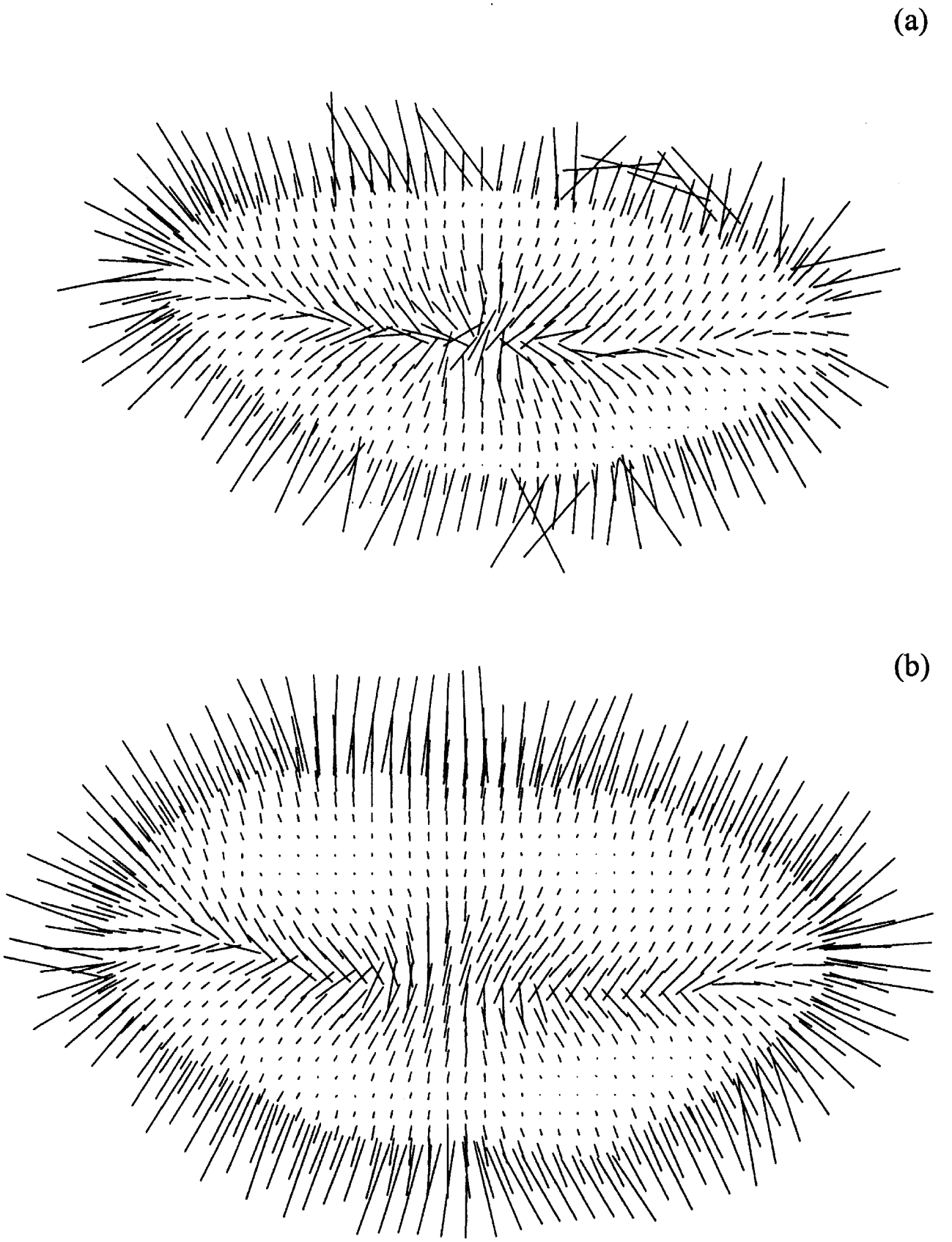

FIG. 7. Quiver plots of the smallest component of the diagonalised diffusion tensor D_{perp} for a 29 year old lens (a) and an 86 year old lens (b).

diffusion coefficient is strongly influenced by the permeability of water through the cell membranes.

The pronounced minimum in D_{perp} within the lens cortex is an evidence of a 'diffusion barrier' restricting the transport of water between the lens surface and the fibre cells of the lens nucleus. These results are consistent with the restriction or barrier to the transport of radio-labelled glutathione (and presumably also other small molecules such as water) between the lens nucleus and cortex reported by Sweeney and Truscott 1998). Such a barrier would also explain the reduced effective diffusion rates for transport of water (^2H_2O) into the lens nucleus we reported previously (Moffat et al., 1999). In some cases, the minimum values of D_{perp} approached the limits of resolution in our experiments (D_{perp} approximately 1×10^{-10} m^2 sec^{-1}).

In order to investigate the changes in dimensions of the barrier with age, the anterior barrier thickness, posterior barrier thickness and the axial distance between the barriers (axial diameter) were measured for several lenses of different ages from profiles similar to those in Fig. 3. The results are presented in Fig. 8 where they are plotted against lens age and compared with the overall axial thickness of the lens. From the linear regression fits, it can be seen that while the overall lens thickness increases significantly ($P < 0{\cdot}0001$, gradient $= 0{\cdot}02$ mm year^{-1}), the anterior barrier thickness and the posterior barrier thickness increase only slightly with age (gradients $= 0{\cdot}01$ and $0{\cdot}005$ mm year^{-1}, respectively). The axial diameter of the barrier, however, does not change significantly ($P = 0{\cdot}2$).

From the profiles of D_{perp}, the mean effective diffusivities of the perpendicular diffusion were also measured for three regions within the diffusion barrier: the anterior section, the posterior section and the equatorial section. These are plotted against age in Fig. 9. The regression results indicate that while the diffusivity in the anterior barrier and posterior barrier are not significantly different, the diffusivity through the equatorial region is significantly faster. There is also no significant ($P > 0{\cdot}1$) change in diffusivities with increasing age above 30

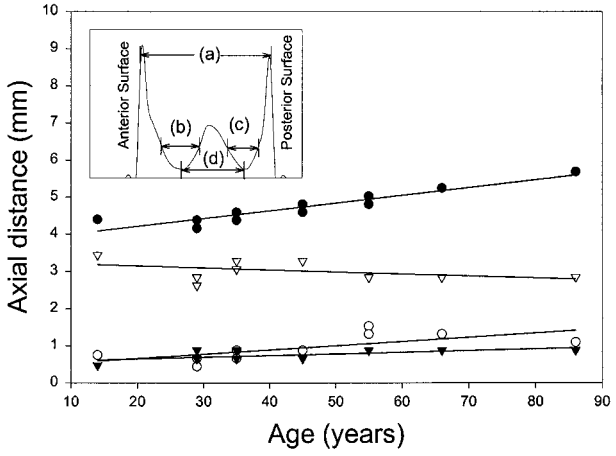

FIG. 8. Dimensions of the diffusion barrier in the axial direction (along the optical axis) compared to the lens axial thickness (see inset for definitions of the plotted parameters). (●) Overall lens thickness (a), (○) anterior thickness of barrier (b), (▼) posterior thickness of barrier (c) and (▽) axial diameter of barrier (d).

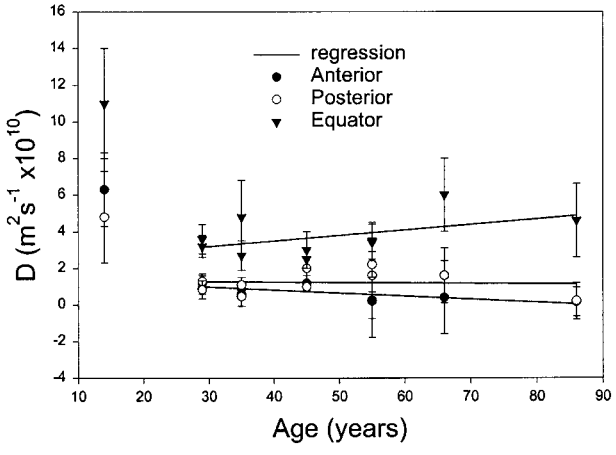

FIG. 9. The mean effective diffusion coefficients at different positions in the diffusion barrier observed in the maps of D_{perp} (Figs. 3 and 7).

years, although it is noticeable that the diffusivities in the barrier region of the 14 year old lens were significantly faster than those measured in the older lenses. (Unfortunately, no further lenses in the age range below 30 years became available during the time course of the project to determine whether this represents an anomalous result.) The higher diffusivities in the equatorial region indicate that there are subtle differences in the lens morphology (on a microscopic scale) that allow faster communication between fibre cells in this region. Such morphological differences could include increased membrane permeability or increased fibre cell thickness and corresponding decreased membrane density. Alternatively, the enhanced transport in the equatorial regions of the lens could result from convective flow through channels that are disordered on the scale of our voxel volumes. However, no evidence for convective flows was observed in our earlier studies of long-range transport in the lens (Moffat et al., 1999).

5. Conclusions

Previous bulk diffusion studies (Haner et al., 1989; Babizhaev et al., 1991) and ADC maps (Cheng et al., 1992; Wu et al., 1993) of water diffusion in human and animal lenses have shown that the eye lens not only exhibits inhomogeneous diffusion, but also diffusion anisotropy. The acquisition of full diffusion tensor maps for the first time in this study reveals the detailed nature of water diffusion in human eye lenses. The diffusion tensor maps show that the lens fibre cells act as channels that facilitate the relatively unrestricted transport of water and other metabolites from the metabolically active epithelial cells at the anterior surface of the lens, to the posterior regions of the lens. This may be a vital property of the lens morphology, which aids in the growth and development of the outer cortical regions and helps to protect the lens crystallins from degradation. In contrast, radial transport involving communication from cell to cell is much more restricted. The diffusion tensor maps show conclusively that the transport of water across cell membranes is highly constrained despite the abundant gap junctions and membrane channels believed to be present in the lens. They also show that inter-cell communication in this direction has a minimum in the vicinity of the nucleus/cortex interface suggesting that there is a decrease in cell thickness in this region and/or a reduction in membrane permeability. This confirms that a barrier to transport of molecules from the cortex to the nucleus and vice versa does indeed exist.

The perpendicular diffusion in the equatorial region of the barrier is much greater than in the anterior and posterior parts of the barrier. This suggests that communication between cells is greatest in this region. Scanning electron microscopy studies (Bron et al., 2000) confirm a decrease in lens cell thickness at the nucleus/cortex interface and also an increase in the gap junction density (Mathias et al., 1997) in the equatorial regions. Decreased perpendicular diffusion at this interface, irrespective of its origin, means that this area controls the rate of transport of all water-soluble metabolites either into or out of the nuclear region. The slow rates of diffusion observed in the barrier explain the slow effective diffusion rates measured previously (Moffat et al., 1999). The age-dependent changes to the barrier seen in Fig. 8 and 9 may also explain the observed reduction with age in the average effective diffusivity for transport of water into/out of the lens nucleus reported in this earlier study and the impediment to GSH diffusion (Sweeney and Truscott, 1998) found in older lenses.

The lens nucleus is the most common site for senile cataract formation. The nucleus has particularly poor communication with the rest of the lens and the outside environment. This lack of communication implies that important anti-oxidants and nutrients in the lens nucleus may be gradually depleted during the ageing process making the lens more susceptible to protein denaturing, precipitation and hence cataract formation. Similarly, the residence time of reactive waste products in the lens nucleus may be increased, leading to protein oxidation or cross-linking and the onset of presbyopia. Conversely, it is also possible that this lack of communication may protect the sensitive metabolically inactive lens nucleus by forming a barrier to cell toxins. Support for this is provided by the fact that cataracts caused by chemical imbalances or toxins mostly result in cortical cataract (Nunnari et al., 1986; Lipman et al., 1988; Harding, 1991; Cheng et al., 1992; Spector, 1995; Bettelheim et al., 1998). The early development of the barrier suggests that the presence of this barrier does not represent a breakdown of lens function, but may be an important morphological property to protect the lens nucleus. However, this may at the same time prevent the efficient replenishment of important nutrients in the lens nucleus and as a result of the ageing process, cause a decrease in content of these important nutrients and anti-oxidants necessary to prevent cataractogenesis.

Acknowledgements

The authors wish to acknowledge support for this project from the Australian Research Council and the Queensland and NSW Eye Banks. One of us (B.A.M) also wishes to thank Queensland University of Technology for a postgraduate research scholarship.

References

Babizhaev, M. A., Nikolaev, G. M., Goriachev, S. I. and Dautova, N. R. (1991). Diffusion properties of water in the human crystalline lens during cataract development. *Biofizika* **36**, 327–9.

Bettelheim, F. A., Li, L. and Zeng, F. F. (1998). Do changes in the hydration of the diabetic human lens precede

cataract formation? *Res. Commun. Mol. Pathol. Pharmacol.* **102**, 3–14.

Bron, A. J., Vrensen, G. F., Koretz, J., Maraini, G. and Harding, J. J. (2000). The ageing lens. *Ophthalmologica* **214**, 86–104.

Cheng, H. M., Gonzalez, R. G., Barnett, P. A., Aguayo, J. B., Wolfe, J. and Chylack, L. T., Jr. (1985). Sorbitol/fructose metabolism in the lens. *Exp. Eye Res.* **40**, 223–9.

Cheng, H. M., Kuan, W. P., Garrido, L., Xiong, J. and Chang, C. (1992). High-resolution MR imaging of water diffusion in the rabbit lens. *Exp. Eye Res.* **54**, 127–32.

Coremans, J., Luypaert, R., Verhelle, F., Stadnik, T. and Osteaux, M. (1994). A method for myelin fiber orientation mapping using diffusion-weighted MR images. *Magn. Reson. Imaging* **12**, 443–54.

Gonzalez, A. M., Sochor, M., Hothersall, J. S. and McLean, P. (1986). Effect of aldose reductase inhibitor (sorbinil) on integration of polyol pathway, pentose phosphate pathway, and glycolytic route in diabetic rat lens. *Diabetes* **35**, 1200–5.

Goodenough, D. A. (1992). The crystalline lens. A system networked by gap junctional intercellular communication. *Semin. Cell Biol.* **3**, 49–58.

Haner, R. L., Schleich, T., Morgan, C. F. and Rydzewski, J. M. (1989). Water self-diffusion in the calf lens. *Exp. Eye Res.* **49**, 371–6.

Harding, J. (1938/1991). *Cataract: Biochemistry, Epidemiology, and Pharmacology/John Harding*, 1st Ed., Chapman and Hall: London.

Hightower, K. R. and Harrison, S. E. (1987). The influence of calcium on glucose metabolism in the rabbit lens. *Invest. Ophthalmol. Vis. Sci.* **28**, 1433–6.

Lipman, R. M., Tripathi, B. J. and Tripathi, R. C. (1988). Cataracts induced by microwave and ionizing radiation. *Surv. Ophthalmol.* **33**, 200–10.

Martin, K. M., Papadakis, N. G., Huang, C. L., Hall, L. D. and Carpenter, T. A. (1999). The reduction of the sorting bias in the eigenvalues of the diffusion tensor. *Magn. Reson. Imaging* **17**, 893–901.

Mathias, R. T., Rae, J. L. and Baldo, G. J. (1997). Physiological properties of the normal lens. *Physiol. Rev.* **77**, 21–50.

Moffat, B. A., Landman, K. A., Truscott, R. J., Sweeney, M. H. and Pope, J. M. (1999). Age-related changes in the kinetics of water transport in normal human lenses. *Exp. Eye Res.* **69**, 663–9.

Morgan, C. F., Schleich, T., Caines, G. H. and Farnsworth, P. N. (1989). Elucidation of intermediate (mobile) and slow (solid-like) protein motions in bovine lens homogenates by carbon-13 NMR spectroscopy. *Biochemistry* **28**, 5065–74.

Nunnari, J. M., Williams, T. R. and Powell, D. L. (1986). Determination of the state and content of water in human normal and cataractous lenses by differential scanning calorimetry. *Ophthalmic Res.* **18**, 117–24.

Obrosova, I., Faller, A., Burgan, J., Ostrow, E. and Williamson, J. R. (1997). Glycolytic pathway, redox state of NAD(P)-couples and energy metabolism in lens in galactose-fed rats: effect of an aldose reductase inhibitor. *Curr. Eye Res.* **16**, 34–43.

Ohtori, A., Yamamoto, Y. and Tojo, K. J. (1991). Penetration and binding of aldose–reductase inhibitors in the lens. *Invest. Ophthalmol. Vis. Sci.* **32**, 189–93.

Paterson, C. A. (1970). Extracellular space of the crystalline lens. *Am. J. Physiol.* **218**, 797–802.

Skare, S., Li, T., Nordell, B. and Ingvar, M. (2000). Noise considerations in the determination of diffusion tensor anisotropy. *Magn. Reson. Imaging* **18**, 659–69.

Spector, A. (1995). Oxidative stress-induced cataract: mechanism of action. *FASEB J.* **9**, 1173–81.

Stejskal, E. O. and Tanner, J. E. (1965). Spin diffusion measurements: spin echoes in the presence of a time-dependent field gradient. *J. Chem. Phys.* **42**, 288–92.

Sweeney, M. H. and Truscott, R. J. (1998). An impediment to glutathione diffusion in older normal human lenses: a possible precondition for nuclear cataract. *Exp. Eye Res.* **67**, 587–95.

Truscott, R. J. and Augusteyn, R. C. (1977). Oxidative changes in human lens proteins during senile nuclear cataract formation. *Biochim. Biophys. Acta* **492**, 43–52.

Tsubota, K., Krauss, J. M., Kenyon, K. R., Laing, R. A., Miglior, S. and Cheng, H. M. (1989). Lens redox fluorometry: pyridine nucleotide fluorescence and analysis of diabetic lens. *Exp. Eye Res.* **49**, 321–34.

Tsubota, K. and Laing, R. A. (1992). Glycolytic oscillation and effect of metabolic inhibitor on rat lens. *Jpn. J. Ophthalmol.* **36**, 265–72.

Wu, J. C., Wong, E. C., Arrindell, E. L., Simons, K. B., Jesmanowicz, A. and Hyde, J. S. (1993). In vivo determination of the anisotropic diffusion of water and the T1 and T2 times in the rabbit lens by high-resolution magnetic resonance imaging. *Invest. Ophthalmol. Vis. Sci.* **34**, 2151–8.